

A REFORMULATION OF THE RIEMANN HYPOTHESIS IN TERMS OF CONTINUITY OF THE LIMIT FUNCTION OF A CERTAIN RATIO OF PARTIAL SUMS OF A SERIES FOR THE DIRICHLET ETA FUNCTION.

LUCA GHISLANZONI

luca.ghislanzoni@fastwebnet.it

ABSTRACT. For any $s \in \mathbb{C}$ with $\Re(s) > 0$, denote by $S_n(s)$ the n^{th} partial sum of the alternating Dirichlet series $1 - 2^{-s} + 3^{-s} - \dots$. We first show that $S_n(s) \neq 0$ for all n greater than some index $N(s)$. Denoting by $D = \{s \in \mathbb{C} : 0 < \Re(s) < \frac{1}{2}\}$ the open left half of the critical strip, define for all $s \in D$ and $n > N(s)$ the ratio $P_n(s) = S_n(1-s)/S_n(s)$. We then prove that the limit $L(s) = \lim_{N(s) < n \rightarrow \infty} P_n(s)$ exists at every point s of the domain D . Finally, we show that the function $L(s)$ is continuous on D if and only if the Riemann Hypothesis is true.

1. INTRODUCTION

On the 11th of August 1859, Bernhard Riemann was appointed member of the Berlin Academy. Respectful of such great honor, Riemann submitted to the Academy his seminal work on the distribution of prime numbers less than a given quantity (Über die Anzahl der Primzahlen unter einer gegebenen Grösse, [1]). In that paper Riemann formulated a daring hypothesis [2]:

All non-trivial zeros of the zeta function lie on the critical line

Denoted by $s = \sigma + it$ a complex number, said Riemann Zeta function, $\zeta(s)$, is the function defined as the analytic continuation to all the complex values $s \neq 1$ of the infinite series:

$$(1) \quad \zeta(s) = \sum_{n=1}^{\infty} \frac{1}{n^s} = 1 + \frac{1}{2^s} + \frac{1}{3^s} + \frac{1}{4^s} + \dots,$$

which converges in the half-plane $\Re(s) > 1$. $\zeta(s)$ has zeros at $s = -2, -4, -6, \dots$, which are called **trivial zeros** because their existence is easy to prove. The Riemann zeta function features also other zeros, called **non-trivial zeros**, known to lie in the open strip $\{s \in \mathbb{C} : 0 < \Re(s) < 1\}$, which is called the **critical strip**. The **critical line** is then defined as the line $\{s \in \mathbb{C} : \Re(s) = \frac{1}{2}\}$. The Riemann Hypothesis asserts that all **non-trivial zeros** have real part $\Re(s) = \frac{1}{2}$.

Since Riemann's milestone paper the properties of $\zeta(s)$ have been studied in much depth, and during the past 150 years a huge amount of literature has gradually built up. Most of what is currently known about $\zeta(s)$ is nowadays freely available on the Web [3] [4] [5] [6] [7]. From the great wealth of existing literature only few key definitions and results will be recalled in this introduction. This work will then concentrate its attention on the behavior of the zeros of $\zeta(s)$ in the interior of the critical strip.

A key role in the analytical continuation of the series (1) is played by the Dirichlet Eta function [8]:

$$(2) \quad \eta(s) = \sum_{n=1}^{\infty} \frac{(-1)^{n-1}}{n^s} = 1 - \frac{1}{2^s} + \frac{1}{3^s} - \frac{1}{4^s} + \dots$$

The above series represents the simplest alternating signs case among Ordinary Dirichlet Series, and it is converging for all s with $\Re(s) > 0$. Its sum, $\eta(s)$, is an analytic function in the corresponding half-plane. Analytic continuation of the infinite series (1) can then be obtained by observing that:

$$(3) \quad \zeta(s) = \frac{\eta(s)}{1 - \frac{1}{2^s}},$$

which is valid for $s \neq 1 + n \cdot \frac{2\pi}{\ln 2} i$ ($n \in \mathbb{Z}$), values at which the denominator vanishes.

The right hand side of (3) is analytic in the region of interest for this work: the interior of the critical strip. Inside such region, the zeros of the Riemann ζ coincide with the zeros of the Dirichlet η function. As the infinite sum (2) converges readily, it makes it easy to graphically represent the path described by the partial sums. For the interested reader, Figures 6 and 7 at the end depict two elementary examples (the second of which corresponds to the sixth known non-trivial zero), useful for familiarizing with the geometric meaning of the partial sums of the infinite series (2).

The infinite sum (2) can be written as

$$(4) \quad \sum_{n=1}^{\infty} \frac{(-1)^{n-1}}{n^s} = \sum_{n=1}^k \frac{(-1)^{n-1}}{n^s} + \sum_{n=k+1}^{\infty} \frac{(-1)^{n-1}}{n^s} = S_k(s) + R_k(s),$$

where $S_k(s)$ is the k^{th} partial sum and $R_k(s)$ the corresponding remainder term. The convergence of (2) implies that

$$\lim_{k \rightarrow \infty} R_k(s) = 0.$$

The terms of the infinite sum (2) are complex numbers, which can be represented by vectors of the form $(-1)^{n-1} \frac{1}{n^\sigma} e^{-it \ln n}$. The line segments making up the paths graphed in Figures 1, 6 and 7, represent said vectors, added up "tip to tail". As it will be better detailed in the proof of **Theorem 1**, while approaching the point of convergence, $\eta(s)$, the path described by the partial sums always ends up following a very simply structured *star-shaped* path (for clarity, only segments from $n=293$ to $n=313$ are shown), characterized by angles between consecutive segments being $< \frac{\pi}{2}$, getting smaller and smaller as n grows larger and larger.

A remarkable functional equation satisfied by $\zeta(s)$ was originally proposed by Euler in 1749, and later proved by Riemann in his 1859 paper [9] [6]

$$(5) \quad \zeta(1-s) = 2(2\pi)^{-s} \cos\left(\frac{\pi s}{2}\right) \Gamma(s) \zeta(s).$$

When studying the behavior of $\zeta(s)$ inside the critical strip, a useful implication of (5) is that to $\zeta(s) = 0$ it must correspond $\zeta(1-s) = 0$. Therefore, if $s = \frac{1}{2} - \alpha + it$ ($0 < \alpha < \frac{1}{2}$) is a zero of $\zeta(s)$, then so it must be for both $1-s = \frac{1}{2} + \alpha - it$ and its complex conjugate $1-\bar{s} = \frac{1}{2} + \alpha + it$. Thus, non-trivial zeros always occur in groups of two pairs, one pair being the complex conjugate of the other. Zeros belonging to the same pair are symmetrical about the critical line. As this work is concerned with the study of the behavior of the zeros of $\zeta(s)$ in the interior of the critical strip, and inside such region a useful implication of (3) is that said zeros coincide with the zeros of $\eta(s)$, one could as well concentrate on the study of the behavior of pairs of *critical line symmetrical zeros* of the function $\eta(s)$. This latter approach has been preferred by the author, as the readily converging sum (2) allows to easily visualize, by drawing the corresponding graphs, the paths described by the partial sums of *critical line symmetrical arguments*.

Much intuition about the geometric behavior of the sequence of partial sums $\{S_k\}$ can be gained by visually inspecting the example graphed in Fig. 1. The depicted pattern of convergence, although referring to particular values of α and t , is in fact very general and representative of the typical behavior. Each segment is defined by

$$(-1)^{n-1} \frac{1}{n^{1/2-\alpha+it}} = (-1)^{n-1} \frac{1}{n^{1/2-\alpha}} e^{-it \ln n}$$

for the path composed of the longer segments (red), and

$$(-1)^{n-1} \frac{1}{n^{1/2+\alpha+it}} = (-1)^{n-1} \frac{1}{n^{1/2+\alpha}} e^{-it \ln n}$$

for the path composed of the shorter segments (green). It is hence clear that the two paths are composed of parallel segments, whose lengths and common value of the angle they form with the real axis are respectively:

$$(6) \quad \frac{1}{n^{\frac{1}{2}-\alpha}} \quad \frac{1}{n^{\frac{1}{2}+\alpha}} \quad \theta_n(t) = \begin{cases} -t \ln n & \text{if } n \text{ is odd} \\ \pi - t \ln n & \text{if } n \text{ is even} \end{cases}$$

Let us now follow the two paths starting from the origin, $0 + i0$. The first segments ($n = 1$) overlap

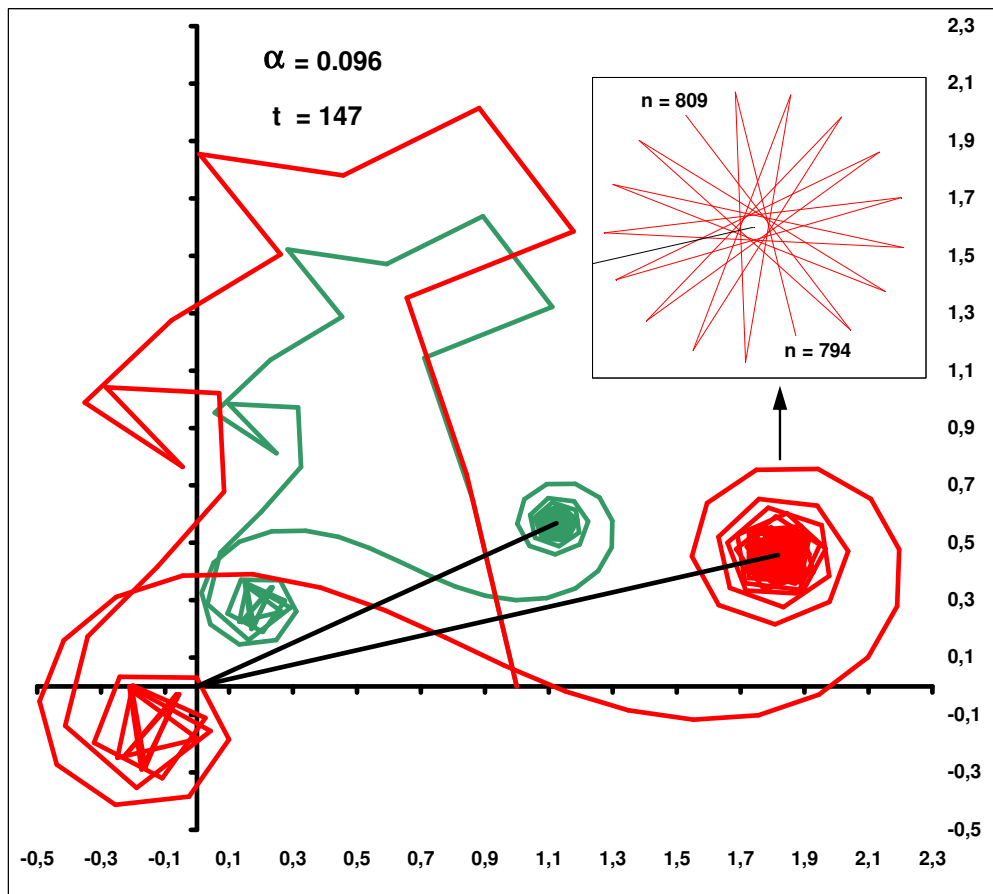


Figure 1: Paths described by the partial sums of the series for $\eta(s)$ and $\eta(1-\bar{s})$, $s = \frac{1}{2} - \alpha + it$.

perfectly, and join the origin with the point $1 + i0$. After the first segment, the n^{th} segment of the path made up of the shorter segments remains parallel to the n^{th} segment of the path made up of the longer segments, although their respective lengths are now related by the factor $n^{-2\alpha}$. Fig. 1 depicts the first 1000 segments. After wandering around the complex plane for the about first hundred segments, both paths settle into a kind of "crisscrossing bound orbit" (those two "tangles", one red, one green, of line segments), eventually converging to the values $\eta(\frac{1}{2} - 0.096 + i147) = 1.816326 + i0.457761$ and $\eta(\frac{1}{2} + 0.096 + i147) = 1.124161 + i0.568465$, respectively. Said points of convergence are identified in Fig. 1 by the segments joining them to the origin. The square inset enlarges a detail of said "crisscrossing bound orbit", as it would appear by zooming deep inside the red "tangle" (although limited to the path from segment 794 to segment 809), revealing that it eventually turns into a very simply structured "star-shaped bound orbit". Furthermore, intuition suggests that the path made up of the shorter segments might well converge to a point closer to the origin than the point of convergence of the path made up of the longer segments. That this is probably the case has been verified over a limited range of t values, by numerically evaluating $|\eta(1-\bar{s})/\eta(s)| = |\eta(\frac{1}{2} + \alpha + it)/\eta(\frac{1}{2} - \alpha + it)|$. The 3D plot of Fig. 2 summarizes the results of said computations. For the interested reader, various 2D sections of the 3D graph of Fig.2 are available in the **Appendix**. For the range of t values studied, it is apparent that $0 \leq |\eta(\frac{1}{2} + \alpha + it)/\eta(\frac{1}{2} - \alpha + it)| \leq 1$, with the equal signs holding only at the boundaries $\alpha = 0$ and $\alpha = \frac{1}{2}$. As it will be proved in the remarks following **Theorem 2**, for fixed t the function depicted in Fig.2 features a nice monotone decreasing behavior along α . Said proof makes use of the results of a study carried out by Saidak and Zvengrowski [10], and concerning the behavior of the ratio of the modulus of Riemann Zeta Function values of critical line symmetrical arguments. The two authors proved that, for $t \geq 2\pi + 1$ and $0 \leq \alpha \leq \frac{1}{2}$, said ratio is a strictly monotone increasing function

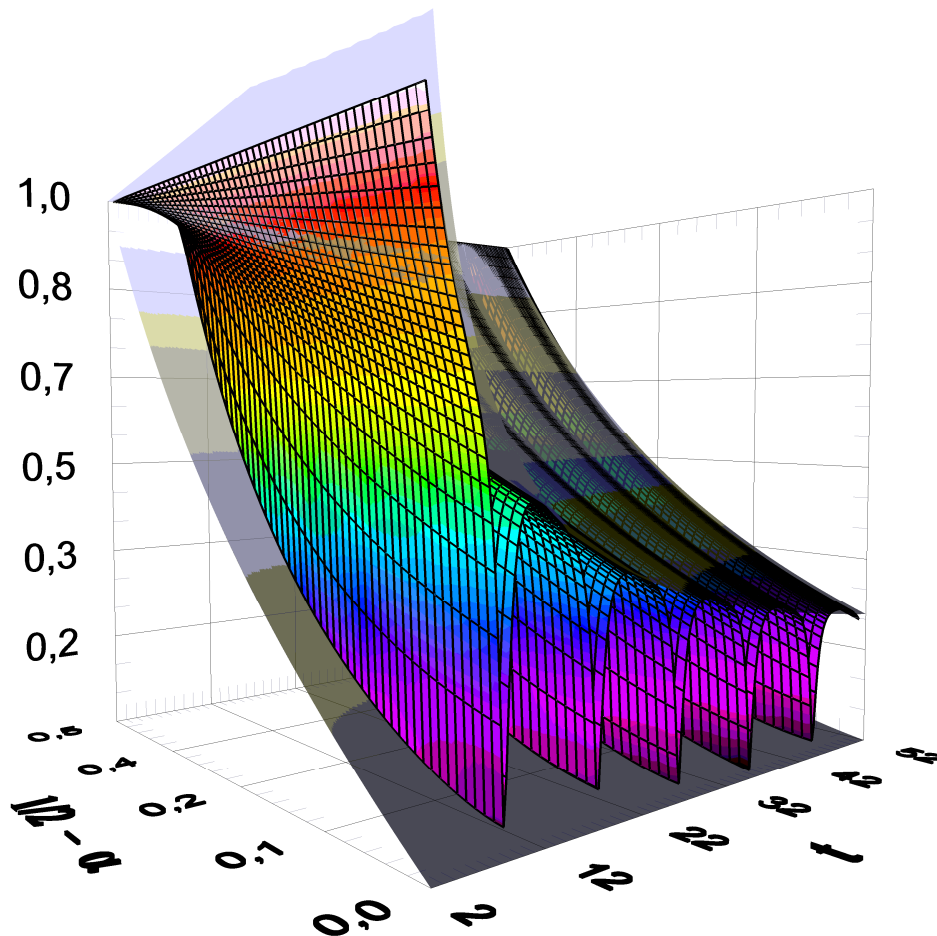


Figure 2: visualizing $\left| \frac{\eta(\frac{1}{2} + \alpha + it)}{\eta(\frac{1}{2} - \alpha + it)} \right|$; upper bound is $(\frac{8\pi}{9t})^\alpha$, lower is $\frac{1-2\alpha}{1+2\alpha} (\frac{8\pi}{9t})^\alpha$.

of α . Concerning estimates for upper and lower bounds of the function depicted in Fig.2, and within the range of values covered by the numerical simulations performed, $0 \leq \alpha \leq \frac{1}{2}$ and $2 \leq t \leq 120$, the author was further able to test the following conjecture:

Conjecture 1. *The following inequalities hold:*

$$(7) \quad \frac{1-2\alpha}{1+2\alpha} (8\pi/9t)^\alpha \leq \left| \frac{\eta(\frac{1}{2} + \alpha + it)}{\eta(\frac{1}{2} - \alpha + it)} \right| \leq (8\pi/9t)^\alpha \quad \left(t \geq 2\pi + 1, \quad 0 \leq \alpha < \frac{1}{2} \right).$$

As this work is concerned with the study of non trivial zeros, the first of which is known to occur at $t = 14,13472514$, choosing to limit the above estimate to values $t \geq 2\pi + 1$ allows easier comparison with the results obtained by Saidak and Zvengrowski, while excluding a region of the critical strip which anyway is known to be void of zeros. The way the estimate for the upper bound was conjectured is based on equality (11) here below. It was first observed that the "wavy" behavior displayed by the function plotted in Fig.2 is mainly due to the contribution of the first factor in (9), whose maxima, along t directions, occur at odd multiples of $\pi/\ln 2$. To estimate the asymptotic behavior, for large t values, the modulus of the first factor in (9) was hence evaluated at said maxima, resulting in $\frac{1+2^\sigma}{1+2^{1-\sigma}}$. The modulus of the second factor is clearly $\frac{2}{(2\pi)^\sigma}$. Finally, the asymptotic behaviors, as $t \rightarrow \infty$, of the modulus of the complex cosine and complex

gamma functions are $|\cos(\frac{\pi}{2}\sigma + i\frac{\pi}{2}t)| \sim \frac{1}{2}e^{\frac{\pi}{2}t}$ and $|\Gamma(\sigma + it)| \sim \sqrt{2\pi} e^{-\frac{\pi}{2}t} t^{\sigma-\frac{1}{2}}$ [13], respectively. Thus

$$\frac{1+2^\sigma}{1+2^{1-\sigma}} \frac{2}{(2\pi)^\sigma} \left| \cos\left(\frac{\pi}{2}\sigma + i\frac{\pi}{2}t\right) \Gamma(\sigma + it) \right| \sim \frac{1+2^\sigma}{1+2^{1-\sigma}} \left(\frac{t}{2\pi}\right)^{\sigma-\frac{1}{2}} \quad \text{as } t \rightarrow \infty .$$

The form of the above estimate can be further simplified by observing that, when $0 \leq \sigma \leq \frac{1}{2}$, there exists a very good approximation of the factor $\frac{1+2^\sigma}{1+2^{1-\sigma}}$, namely: $\frac{1+2^\sigma}{1+2^{1-\sigma}} \leq \left(\frac{4}{9}\right)^{\frac{1}{2}-\sigma}$. The equal sign holds at the boundaries $\sigma = 0$ and $\sigma = \frac{1}{2}$, while the maximum absolute deviation is $1.75 \cdot 10^{-4}$. Thus, by setting $\sigma = \frac{1}{2} - \alpha$ we finally obtain the upper bound in (7). Indeed, the so conjectured upper bound appears to represent a pretty good estimate (see Fig.5) even at t values as low as $\pi/\ln 2$. Concerning the lower bound, the modulus of the first factor in (9) was evaluated at its minima, occurring at even multiples of $\pi/\ln 2$, resulting in $\frac{1-2^\sigma}{1-2^{1-\sigma}}$. Few trial and error attempts in term of elementary functions allowed then to verify the following approximation: $\frac{1-2^\sigma}{1-2^{1-\sigma}} \left(\frac{4}{9}\right)^{\frac{1}{2}-\sigma} \leq \frac{1-2^\sigma}{1-2^{1-\sigma}}$, where the equal sign holds at the boundaries $\sigma = 0$ and $\sigma = \frac{1}{2}$, while the maximum absolute deviation is $5.75 \cdot 10^{-3}$. The proposed lower bound estimate is not as accurate as the one for the upper bound (see Fig.5c), although quite reasonable. As for what concerns the scope of this work, the weaker inequality $|P(s)| > 0$ will be sufficient. We now recall some useful relationships

$$(8) \quad \left| \eta\left(\frac{1}{2} + \alpha + it\right) \right| = \left| \overline{\eta\left(\frac{1}{2} + \alpha + it\right)} \right| = \left| \eta\left(\frac{1}{2} + \alpha - it\right) \right| = \left| \eta\left(1 - \left(\frac{1}{2} - \alpha + it\right)\right) \right|,$$

that, by applying the substitution $s = \frac{1}{2} - \alpha + it$, we will use to reformulate in a more conventional notation the function plotted in Fig.2. Let us first define the following function

$$(9) \quad P(s) = \frac{1-2^s}{1-2^{1-s}} 2(2\pi)^{-s} \cos\left(\frac{\pi}{2}s\right) \Gamma(s) ,$$

on a domain coinciding with the critical strip. Recalling (3) and (5), we have

$$(10) \quad \frac{\eta(1-s)}{\eta(s)} = P(s) \quad \text{when } \eta(s) \neq 0 .$$

By further noting that $|\eta(1-\bar{s})| = |\eta(1-s)|$, for the function plotted in Fig.2 we finally have

$$(11) \quad \frac{\left| \eta\left(\frac{1}{2} + \alpha + it\right) \right|}{\left| \eta\left(\frac{1}{2} - \alpha + it\right) \right|} = \left| \frac{\eta(1-s)}{\eta(s)} \right| = |P(s)| > 0 \quad \text{when } \eta(s) \neq 0 .$$

It is interesting to remark that along the critical line it is $|P(\frac{1}{2} + it)| = 1$ (see also the first remark following **Theorem 2**). The function $|P(s)|$ behaves nicely, displaying a monotonically decreasing behavior along α (note that $\alpha = \frac{1}{2} - \Re(s)$). In the remarks following **Theorem 2** it will be proved that the observed monotonically decreasing behavior holds for all values $t \geq 1 + 2\pi$.

A further very useful and informing intuition, gathered by observing in Fig. 1 the path drawn by the partial sums, is the following: once said path gets "trapped" into a *star-shaped orbit* (inset of Fig.1), it appears as the distance between the point of convergence, $\eta(s)$, and the partial sum $S_n(s)$ is roughly of the same order of magnitude as the length, $n^{-\sigma}$, of its last segment. That this is indeed the case is the subject of **Theorem 1**. The demonstration of **Theorem 2** will then take advantage of a trivial implication of (4), namely

$$(12) \quad \eta(s) = 0 \quad \Rightarrow \quad R_n(s) = -S_n(s) ,$$

(for the reader wishing to graphically visualize this trivial observation, see in Fig. 7 the example referring to R_{292} and S_{292}). By the very definition of $\eta(s)$, a straightforward implication of **Corollary 1.1** is then

$$(13) \quad \eta(s) = 0 \quad \Rightarrow \quad \lim_{n_o(s) < n \rightarrow \infty} \frac{S_n(1-s)}{S_n(s)} = \lim_{n_o(s) < n \rightarrow \infty} \frac{R_n(1-s)}{R_n(s)} = 0 .$$

Defining

$$P_n(s) = \frac{S_n(1-s)}{S_n(s)},$$

Corollary 1.3 will further prove that the limit function $L(s) = \lim_{N(s) < n \rightarrow \infty} P_n(s)$ exists for all s in the open left half of the critical strip. It then appears that the sequence of functions $\{P_n(s)\}$ would in such case converge to $P(s)$, except at values s corresponding to hypothetical zeros located off the critical line, and where it would instead vanish. The limit function would hence be discontinuous, vanishing at the locations of said zeros, but with values $P(s) \neq 0$ everywhere else on its domain. However, were the Riemann Hypothesis true, the sequence $\{P_n(s)\}$ would converge to the continuous function $P(s)$ without introducing discontinuities.

The results of the numerical simulations that the author was able to carry out suggest that the strictly monotone decreasing behavior (versus $\alpha = \frac{1}{2} - \Re(s)$) of $|P(s)|$ is mirrored by a similar behavior of the ratios $|P_n(s)|$, at least eventually as $n \rightarrow \infty$ (see an example in Fig. 9a). In other words, the ratios $|P_n(s)|$ appear to converge to $|P(s)|$ without displaying any kind of *wiggling* behavior (as it would, for example, be the case for partial sums of Fourier type of series, *wiggling* around their limit function while converging towards it). Therefore, we are lead to expect that the existence of zeros lying off the critical line would result in a pattern of convergence probably not too dissimilar from the one illustrated in Fig.9b: the solid black line represents $|P(s)|$, a pair of hypothetical zeros are located at $\alpha = 0.15$, the green, red, and blue lines are intended to represent generic ratios $|P_n(s)|$ of order $m < n < o$ respectively. A *non-uniform* pattern of convergence would hence display a sharp deep, narrowing more and more as $n \rightarrow \infty$, while its value at $\alpha = 0.15$ would $\rightarrow 0$.

The above considerations lead naturally to the study of the properties of convergence of the sequence $\{P_n(s)\}$. In the half plane $\Re(s) \geq \varepsilon > 0$, with $\varepsilon > 0$ no matter how small, the sequence of the partial sums of η , $\{S_n(s)\}$, is known to be *locally uniformly convergent* [14]. Furthermore, each $S_n(s)$ is a continuous function. A look at the pattern of convergence of the $S_n(s)$, as depicted for example in figures 6 and 7, shall make it clear that $S_n(s) \neq 0$ for *almost all* n (this will be the subject of various Corollaries at the end of **Theorem 1**), so implying that the ratio $S_n(1-s)/S_n(s)$ is also a continuous function for *almost all* n . It is now useful to recall that if a sequence of functions $\{f_n(x)\}$ is locally uniformly convergent to $f(x)$ and the $f_n(x)$ are continuous at x_0 for *almost all* n , then also the limit function $f(x)$ is continuous at x_0 . However, the locally uniform convergence of $\{S_n(1-s)\}$ and $\{S_n(s)\}$ is in general not sufficient to imply the locally uniform convergence of their ratio.

In the absence of further information about the convergence behavior of the sequence of functions $\{P_n(s)\}$ it is nevertheless interesting to study what the implications would be of making the assumption that its limit function $L(s)$ is indeed continuous. **Theorem 2** will demonstrate that said assumption is both a necessary and sufficient condition for the Riemann Hypothesis to hold true. It therefore represents a statement equivalent to the Riemann Hypothesis.

2. THE GEOMETRIC APPROACH

In the following we will make use of the so-called Big-Theta notation. We therefore recall its definition, in the form which we will be using.

Let $f(n)$ and $g(n)$ be two functions defined on \mathbb{Z}_+ . We say that $f(n)$ is $\Theta(g(n))$ if there exist $C1, C2 \in \mathbb{R}^+$ and $m \in \mathbb{N}$, such that

$$\forall n > m \quad C1 |g(n)| \leq |f(n)| \leq C2 |g(n)|$$

Big-Theta, giving an asymptotic *equivalence*, describes therefore a stronger asymptotic condition than the one described by Big-O, which gives only an asymptotic *upper bound*. In the following proof we will make extensive use also of the Big-O notation, noting that when the use of Big-Theta is not strictly necessary we will conform to the common habit of using Big-O, even in those instances that we know to be characterized by a Big-Theta type of asymptotic behavior. So, taking the example of $f(n) = 7n^{-1} + 2n^{-2} + 11n^{-3}$, it is

clear how $f(n) = \Theta(n^{-1})$, as $n \rightarrow \infty$, although using $O(n^{-1})$ is also understood to be as effective for what concerns its application to the asymptotic analyses that follow later in this proof.

Theorem 1. *In the half plane $\sigma > 0$ let $R_n(\sigma + it)$ be the n^{th} remainder of the infinite series for $\eta(\sigma + it)$. Chosen an $0 < \varepsilon < 1$, no matter how small, we have*

$$(14) \quad \exists m = m(\sigma, \varepsilon) \in \mathbb{Z}_+ : \forall n > m \quad \frac{1 - \varepsilon}{2n^\sigma} < |R_n(\sigma + it)| < \frac{1}{n^\sigma} .$$

In other words, $R_n(\sigma + it) = \Theta(n^{-\sigma})$ as $n \rightarrow \infty$.

PROOF. The procedure followed for this proof is based on a geometric analysis of the pattern of convergence displayed by the path described by the partial sums $S_n(s)$. Said path is composed of line segments, and we will use the term *segment n* to refer to the line segment with endpoints $S_{n-1}(s)$ and $S_n(s)$. Furthermore, because pair of paths corresponding to $s = \sigma + it$ and $\bar{s} = \sigma - it$ are mirror symmetrical with respect to the real axis, it will be sufficient to prove the following results for $t \geq 0$.

While approaching their respective point of convergence, $\eta(s)$, paths corresponding to different values of $\sigma > 0$ appear all to end up describing simply structured *star-shaped patterns*, characterized by angles between consecutive segments being $< \frac{\pi}{2}$. This is actually the result of having to add π , to the argument $-t \ln(n)$, every other segment (because of the alternating sign). In fact, when n becomes sufficiently large, $t \ln(n+1)$ will be just a bit larger than $t \ln(n)$, and because one of the two segments will need to be turned around by π (the segment corresponding to even n), the angle between said consecutive segments will eventually become an acute angle $\delta_{n+1} = t \ln(n+1) - t \ln(n) < \frac{\pi}{2}$ (Fig. 8a helps in visualizing this), shrinking down more and more as n grows larger and larger. Being interested solely in the absolute value of said acute angle, it can be easily verified that its value is $|-t \ln \frac{n+1}{n}| = |t \ln \frac{n+1}{n}|$, which is the same as $t \ln \frac{n+1}{n}$ when $t \geq 0$, and hence $\rightarrow 0$ as $n \rightarrow \infty$. Ultimately, the observed star-shaped pattern is a direct result of the alternating signs in (2).

Fig. 3 illustrates an example, limited to just 3 consecutive segments, of how said pattern appears once the path described by the partial sums has already settled into a *star-shaped orbit*. Of course, we will at first need to demonstrate that said *star-shaped orbit* corresponds to a "bound" orbit. To this end we construct a circle whose diameter is *segment n* , and whose center, C_n , is the midpoint of said *segment n* . Then, if the disk defined by the circle constructed in a similar way on *segment $n+2$* were eventually (i.e.: as $n \rightarrow \infty$) contained within the disk defined by the circle constructed on *segment n* , we would have proved that the distance between point $S_n(s)$ and the point of convergence, $\eta(s)$, cannot be greater than the length of *segment n* . Fig. 3a illustrates the geometric construction on which this proof will be based.

As this proof is concerned solely with the geometric relationships of *segment n* , *segment $n+1$* , and *segment $n+2$* , relatively to each other, the *System of Reference* can be chosen in any convenient way which preserves said relative properties. The origin of the system of coordinates chosen for Fig.3 coincides with the point $S_n(s)$, while the real axis is chosen as to overlap *segment n* . In Fig. 3b the scale of the imaginary axis has been stretched by a factor of 10, only to make it easier to visualize the pattern described by the partial sums. Referring to the triangle defined by the intersections of *segment n* , *segment $n+1$* , and *segment $n+2$* , let us denote by $\delta_{n+1} = t \ln \frac{n+1}{n}$ the angle between *segment $n+1$* and *segment n* , by $\delta_{n+2} = t \ln \frac{n+2}{n+1}$ the angle between *segment $n+2$* and *segment $n+1$* , and by β the supplement of the third angle of said triangle. By construction, angle β corresponds to $\beta = \delta_{n+1} + \delta_{n+2} = t \ln \frac{n+2}{n}$.

Fig. 3b shall then be read as follows:

segment n starts off at $\frac{1}{n^\sigma} + i0$, ending at $0 + i0$;

segment $n+1$ starts off at $0 + i0$, ending at $\frac{1}{(n+1)^\sigma} (\cos \delta_{n+1} - i \sin \delta_{n+1})$;

segment $n+2$ starts from the end of *segment $n+1$* , ending at $\frac{\cos \delta_{n+1}}{(n+1)^\sigma} - \frac{\cos \beta}{(n+2)^\sigma} + i \left(-\frac{\sin \delta_{n+1}}{(n+1)^\sigma} + \frac{\sin \beta}{(n+2)^\sigma} \right)$.

Line **A** is drawn through C_n and C_{n+2} , the midpoints of *segment n* and *segment $n+2$* (see the enlarged detail in Fig. 3b). C_n is also the center of the circle (solid line) having *segment n* as its diameter, and hence the radius of said circle is $r_n = \frac{1}{2n^\sigma}$. C_{n+2} is also the center of the circle (dotted line) having *segment $n+2$* as its diameter, and hence the radius of said circle is $r_{n+2} = \frac{1}{2(n+2)^\sigma}$. The purpose of line **A** is to make it

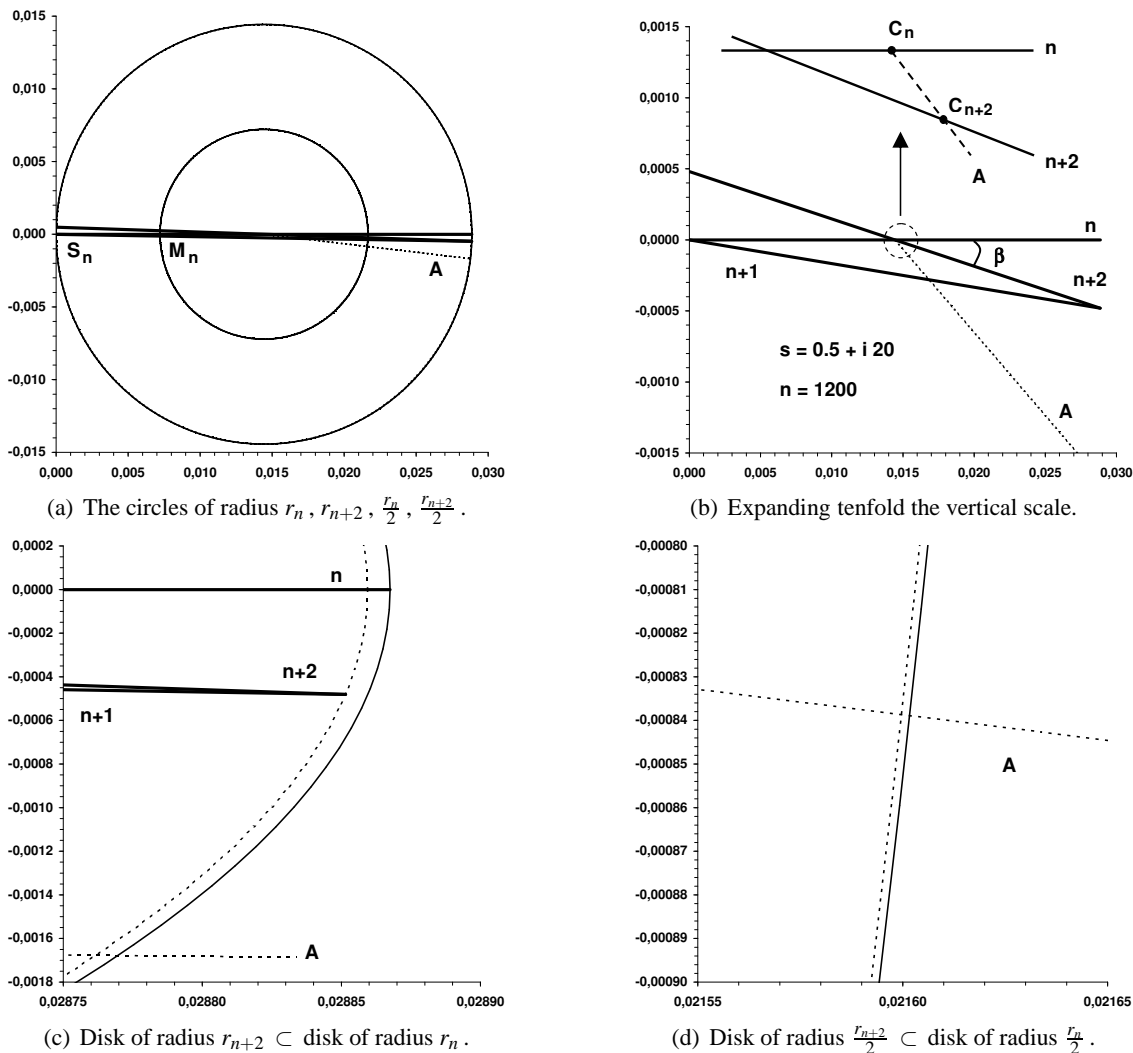


Figure 3: proving that $R_n(\sigma + it)$ is $\Theta(\frac{1}{n^\sigma})$ as $n \rightarrow \infty$.

easier to identify the points of closest approach of the two circles. In Fig. 3c said circles appear stretched. This is the result of having chosen different scale factors for the two axes, so that line **A** may also appear in the graph together with all other segments. It is clear that for the example of Fig.3 ($s = \frac{1}{2} + i20$, $n = 1200$) the disk of radius r_{1202} is contained within the disk of radius r_{1200} (closest approach is their distance along line **A**). Several other examples were verified by numerical simulations, always resulting in *disk* $n + 2$ being eventually contained strictly inside *disk* n , and therefore suggesting that this kind of asymptotic behavior might indeed be representative of the most general case. To demonstrate that this is actually the case, any effective proof will need to rely solely on assumptions eventually satisfied, as $n \rightarrow \infty$, by all the partial sums $S_n(\sigma + it)$, regardless of any particular value $\sigma > 0$. As a matter of fact, for values n such that $t \ln \frac{n+1}{n} < \frac{\pi}{2}$, any three consecutive segments will define a triangle of the same kind as the one depicted in Fig. 3b, and this irrespective of the particular value $\sigma > 0$ (more precisely, the triangle in Fig.3b actually refers to δ_{n+1} and δ_{n+2} both $< \frac{\pi}{4}$, but it is easy to verify that (15), identifying the locations of C_n and C_{n+2} , are valid even when said angles are both just a tiny little bit less than $\frac{\pi}{2}$). We shall also remark that triangles starting from a *segment* n of odd or even index would be drawn in different *Systems of Reference*. In Fig.3b it is $n = 1200$, and the resulting triangle appears in the fourth quadrant. Had we started from $n = 1201$, the resulting triangle would have appeared in the first quadrant (sort of symmetrical about the real axis with respect to the one

drawn in Fig. 3b) of a different *System of Reference*. In any case, it is clear that the validity of the following proof cannot possibly be affected by our choice to start from a line segment of even index, rather than from one of odd index.

The following proof will refer solely to values $n \geq N$, where $N = N(t)$ is the smallest integer that is not less than $1/(e^{\frac{\pi}{2t}} - 1)$. Let us first evaluate the distance $\Delta_c = \Delta_c(n) = |C_{n+2} - C_n|$

$$(15) \quad C_n = \frac{1}{2n^\sigma} + i0 \quad C_{n+2} = \frac{\cos \delta_{n+1}}{(n+1)^\sigma} - \frac{\cos \beta}{2(n+2)^\sigma} + i \left(-\frac{\sin \delta_{n+1}}{(n+1)^\sigma} + \frac{\sin \beta}{2(n+2)^\sigma} \right)$$

$$(16) \quad \begin{aligned} \Delta_c^2 &= |C_{n+2} - C_n|^2 = \\ &= \frac{\cos^2 \delta_{n+1}}{(n+1)^{2\sigma}} + \frac{\cos^2 \beta}{4(n+2)^{2\sigma}} - \frac{\cos \delta_{n+1} \cos \beta}{(n+1)^\sigma (n+2)^\sigma} + \frac{1}{4n^{2\sigma}} + \frac{\cos \beta}{2n^\sigma (n+2)^\sigma} - \frac{\cos \delta_{n+1}}{n^\sigma (n+1)^\sigma} \\ &+ \frac{\sin^2 \delta_{n+1}}{(n+1)^{2\sigma}} + \frac{\sin^2 \beta}{4(n+2)^{2\sigma}} - \frac{\sin \delta_{n+1} \sin \beta}{(n+1)^\sigma (n+2)^\sigma} \\ &= \frac{1}{(n+1)^{2\sigma}} + \frac{1}{4(n+2)^{2\sigma}} - \frac{\cos(\beta - \delta_{n+1})}{(n+1)^\sigma (n+2)^\sigma} + \frac{1}{4n^{2\sigma}} + \frac{\cos \beta}{2n^\sigma (n+2)^\sigma} - \frac{\cos \delta_{n+1}}{n^\sigma (n+1)^\sigma} . \end{aligned}$$

The arguments of the three cosine terms $\rightarrow 0$, as $n \rightarrow \infty$, hence

$$\begin{aligned} \cos(\beta - \delta_{n+1}) &= \cos \left(t \ln \frac{n+2}{n+1} \right) = 1 - \frac{1}{2} \left(\frac{t}{n+1} \right)^2 + O \left(\frac{1}{n^3} \right) \\ \cos(\beta) &= \cos \left(t \ln \frac{n+2}{n} \right) = 1 - \frac{1}{2} \left(\frac{2t}{n} \right)^2 + O \left(\frac{1}{n^3} \right) \\ \cos(\delta_{n+1}) &= \cos \left(t \ln \frac{n+1}{n} \right) = 1 - \frac{1}{2} \left(\frac{t}{n} \right)^2 + O \left(\frac{1}{n^3} \right) . \end{aligned}$$

For the difference between the two radiuses, $\Delta_r = \Delta_r(n) = |r_n - r_{n+2}|$, we have

$$(17) \quad \Delta_r^2 = \frac{1}{4n^{2\sigma}} + \frac{1}{4(n+2)^{2\sigma}} - \frac{1}{2n^\sigma (n+2)^\sigma} .$$

Subtracting (16) from (17) and simplifying, $\Delta_r^2 - \Delta_c^2$ becomes

$$(18) \quad \frac{(n+1)^\sigma \left[(n+2)^\sigma \cos(\delta_{n+1}) - (n+1)^\sigma \frac{1+\cos(\beta)}{2} \right] - n^\sigma \left[(n+2)^\sigma - (n+1)^\sigma \cos(\beta - \delta_{n+1}) \right]}{n^\sigma (n+1)^{2\sigma} (n+2)^\sigma} .$$

Considering that for any given t the cosine factors $\rightarrow 1$ as $n \rightarrow \infty$, there are good chances that the numerator of (18) might eventually become a strictly positive quantity (that this is actually the case will be proved by means of the asymptotic analysis which follows here below). Hence suggesting that the quantity $\Delta_r^2 - \Delta_c^2$ is eventually > 0 , implying that Δ_r is eventually $\Delta_r > \Delta_c$, in turn implying that the disk defined by *segment* $n+2$ is eventually contained within the disk defined *segment* n . To aid in visualizing how a typical transition to strictly positive values takes place, the example of Fig. 8b plots the expression at the numerator of (18) for $s = 0.50567 + i37.58631$. In such particular example, the transition to positive values occurs at $n = 1398$.

It is now useful to summarize the results obtained so far:

- (1) as $n \rightarrow \infty$ the angle between consecutive segments will eventually become $< \frac{\pi}{2}$
- (2) once the above condition is reached, eqn. (16) yields the exact value of $|C_{n+2} - C_n|^2$
- (3) the expression at the numerator of (18) can then be used to compute the exact value of the index $n_o(s)$ such that $\forall n > n_o(s) \Rightarrow \Delta_r > \Delta_c$.

Besides being able to compute said index $n_o(s)$, we need to verify the asymptotic behavior of the sign of the quantity $\Delta_r^2 - \Delta_c^2$. Substituting for the cosine terms their asymptotic expressions

$$\begin{aligned}
 (19) \quad & \Delta_r^2 - \Delta_c^2 = \\
 & = \frac{1}{(n+1)^\sigma (n+2)^\sigma} \frac{[(n+2)^\sigma - (n+1)^\sigma] [(n+1)^\sigma - n^\sigma]}{n^\sigma (n+1)^\sigma} \\
 (20) \quad & + \frac{1}{(n+1)^\sigma (n+2)^\sigma} \frac{(n+1)^\sigma \left[\frac{t^2}{n^2} (n+1)^\sigma - \frac{1}{2} \frac{t^2}{n^2} (n+2)^\sigma - \frac{t^2 n^\sigma}{2(n+1)^2} + O\left(\frac{1}{n^3}\right) \right]}{n^\sigma (n+1)^\sigma}.
 \end{aligned}$$

Term (19) can be further simplified to

$$(21) \quad \frac{\left[\left(1 + \frac{1}{n+1}\right)^\sigma - 1 \right] \left[\left(1 + \frac{1}{n}\right)^\sigma - 1 \right]}{(n+1)^\sigma (n+2)^\sigma} = \frac{1}{(n+1)^\sigma (n+2)^\sigma} \left[\frac{\sigma^2}{n(n+1)} + O\left(\frac{1}{n^3}\right) \right],$$

where a MacLaurin series expansion has been applied to the factors at the numerator. Further simplifying term (20) yields instead

$$\begin{aligned}
 & \frac{1}{(n+1)^\sigma (n+2)^\sigma} \frac{t^2}{2n^2} \left[2 \left(1 + \frac{1}{n}\right)^\sigma - \left(1 + \frac{2}{n}\right)^\sigma - \frac{n^2}{(n+1)^2} + O\left(\frac{1}{n}\right) \right] \\
 = & \frac{1}{(n+1)^\sigma (n+2)^\sigma} \frac{t^2}{2n^2} \left[2 \left(1 + \frac{\sigma}{n} + O\left(\frac{1}{n^2}\right)\right) - \left(1 + \frac{2\sigma}{n} + O\left(\frac{1}{n^2}\right)\right) - \frac{n^2}{(n+1)^2} + O\left(\frac{1}{n}\right) \right] \\
 = & \frac{1}{(n+1)^\sigma (n+2)^\sigma} \frac{t^2}{2n^2} \left[\frac{1+2n}{(n+1)^2} + O\left(\frac{1}{n}\right) \right] = \frac{1}{(n+1)^\sigma (n+2)^\sigma} \left[O\left(\frac{1}{n^3}\right) \right] \text{ as } n \rightarrow \infty.
 \end{aligned}$$

It is hence clear that (21), as $n \rightarrow \infty$, is the dominant term in $\Delta_r^2 - \Delta_c^2$. Therefore

$$\lim_{n \rightarrow \infty} (\Delta_r^2 - \Delta_c^2) = \lim_{n \rightarrow \infty} \left[\frac{1}{(n+1)^\sigma (n+2)^\sigma} \left(\frac{\sigma^2}{n(n+1)} + O\left(\frac{1}{n^3}\right) \right) \right] = 0^+,$$

meaning that it is eventually a positive quantity, and therefore also implying that $\Delta_r > \Delta_c$ must eventually hold as $n \rightarrow \infty$. In other words: the disk having *segment* $n+2$ as its diameter is eventually contained within the disk having *segment* n as its diameter. So it is also for disk $n+4$, contained within disk $n+2$, disk $n+6$, contained within disk $n+4$, and so on, until said diameter becomes vanishingly small, as $n \rightarrow \infty$, while shrinking down to the point of convergence, $\eta(s)$. Besides identifying the asymptotic behavior, as $n \rightarrow \infty$, of $\Delta_r^2 - \Delta_c^2$, this last result confirms that there must exist an index $n_o(s) > 0$ such that for $\forall n > n_o(s)$ the distance $|R_n(s)|$ between the partial sum $S_n(s)$ and the point of convergence, $\eta(s)$, cannot be greater than the diameter $2r_n = \frac{1}{n^\sigma}$, and hence confirming that the mentioned *star-shaped orbit* must indeed be eventually "*bound*". It has thereby been proven also for the general case what was already visually apparent for the particular examples of Fig.1 and Fig.3, namely

$$(22) \quad \exists n_o = n_o(s) \in \mathbb{Z}^+ : \quad \forall n > n_o \quad |R_n(\sigma + it)| < \frac{1}{n^\sigma}.$$

It can now be verified that a similar result holds also for the circles still centered at C_n and C_{n+2} , but of half the radius. Referring to Fig.3a, M_n indicates one of the two points of intersection with *segment* n of the circle of radius $\frac{r_n}{2}$ (solid line). The aim is to verify that the disk of radius $\frac{r_{n+2}}{2}$ (dotted line) is eventually contained inside the disk $\frac{r_n}{2}$. We therefore need to study the asymptotic behavior of

$$(23) \quad \Delta_{r/2}^2 - \Delta_c^2 = \left| \frac{r_n}{2} - \frac{r_{n+2}}{2} \right|^2 - \Delta_c^2 = \Delta_r^2 - \Delta_c^2 - \frac{3}{4} \Delta_r^2.$$

By observing that

$$-\frac{3}{4} \Delta_r^2 = -\frac{3}{16} \frac{\left[\left(1 + \frac{2}{n}\right)^\sigma - 1 \right]^2}{(n+2)^{2\sigma}} = \frac{1}{(n+2)^{2\sigma}} \left[-\frac{3}{4} \frac{\sigma^2}{n^2} + O\left(\frac{1}{n^3}\right) \right],$$

obtained by applying MacLaurin series expansion to the term in square brackets, we can substitute it back into (23), together with the result previously obtained for $\Delta_r^2 - \Delta_c^2$.

$$\begin{aligned} \Delta_{r/2}^2 - \Delta_c^2 &= \frac{1}{(n+2)^{2\sigma}} \left[\sigma^2 \frac{(n+2)^\sigma}{n(n+1)(n+1)^\sigma} - \frac{3}{4} \frac{\sigma^2}{n^2} + O\left(\frac{1}{n^3}\right) \right] \\ &= \frac{1}{(n+2)^{2\sigma}} \left[\sigma^2 \frac{\left(1 + \frac{1}{n+1}\right)^\sigma}{n(n+1)} - \frac{3}{4} \frac{\sigma^2}{n} + O\left(\frac{1}{n^3}\right) \right] \\ &= \frac{1}{(n+2)^{2\sigma}} \left[\sigma^2 \frac{1 + \frac{\sigma}{n+1} - \frac{3}{4} - \frac{3}{4n} + O\left(\frac{1}{n^2}\right)}{n(n+1)} + O\left(\frac{1}{n^3}\right) \right] \\ &= \frac{1}{(n+2)^{2\sigma}} \left[\frac{\sigma^2}{4n(n+1)} + O\left(\frac{1}{n^3}\right) \right]. \end{aligned}$$

Thereby confirming that also for the circles of half radius it holds

$$(24) \quad \lim_{n \rightarrow \infty} (\Delta_{r/2}^2 - \Delta_c^2) = \lim_{n \rightarrow \infty} \left[\frac{1}{(n+2)^{2\sigma}} \left(\frac{\sigma^2}{4n(n+1)} + O\left(\frac{1}{n^3}\right) \right) \right] = 0^+,$$

meaning that it is eventually a positive quantity, and therefore also implying that $\Delta_{r/2} > \Delta_c$ must eventually hold as $n \rightarrow \infty$. This implies that the disk of radius $\frac{r_{n+2}}{2}$ is eventually contained within the disk $\frac{r_n}{2}$, the disk of radius $\frac{r_{n+4}}{2}$ within the disk $\frac{r_{n+2}}{2}$ and so on, until said radius vanishes, as $n \rightarrow \infty$, while shrinking down to the point of convergence $\eta(s)$. Clearly, this result implies that there must exist an index $j(s) > 0$ such that for $\forall n > j$ the distance $|R_n(s)|$ between the partial sum $S_n(s)$ and the point of convergence, $\eta(s)$, cannot be less than the distance $|S_n(s) - M_n(s)| = \frac{r_n}{2} = \frac{1}{4n^\sigma}$. It has thereby been proven also for the general case what was already visually apparent for the particular examples of Fig.1 and Fig.3, namely

$$\exists j = j(s) \in \mathbb{Z}^+ : \forall n > j \quad |R_n(\sigma + it)| > \frac{1}{4n^\sigma}.$$

We can now remark how the above inequality could be widened in scope. As a matter of fact, whether we choose to draw a circle of radius $\frac{r_n}{2}$, or $\frac{r_n}{100}$, or $\frac{r_n}{1000}$, (remember that by r_n we mean half the length of *segment* n) and so on, the corresponding asymptotic behaviors will result in limit expressions similar to (24). In other words, if we replace the $\frac{1}{2}$ in $\frac{r_n}{2}$ by any $\varepsilon > 0$, no matter how small, we will still be able to find an index $j(s)$ such that for all $n > j$ the disk of radius εr_{n+2} is eventually contained within the disk εr_n , the disk of radius εr_{n+4} within the disk εr_{n+2} , and so on, until said radius vanishes, as $n \rightarrow \infty$, while shrinking down to the point of convergence, $\eta(s)$. Indeed, it is straightforward to verify how (23) above will in such case become

$$\Delta_{r/2}^2 - \Delta_c^2 = \Delta_r^2 - \Delta_c^2 - (1 - \varepsilon^2) \Delta_r^2,$$

while the limit operation (24) changes to

$$\lim_{n \rightarrow \infty} (\Delta_{\varepsilon r}^2 - \Delta_c^2) = \lim_{n \rightarrow \infty} \left[\frac{1}{(n+2)^{2\sigma}} \left(\frac{\varepsilon^2 \sigma^2}{n(n+1)} + O\left(\frac{1}{n^3}\right) \right) \right] = 0^+.$$

We can therefore state that chosen an $0 < \varepsilon < 1$, no matter how small, the following inequality holds

$$(25) \quad \exists j = j(s) \in \mathbb{Z}^+ : \forall n > j \quad |R_n(\sigma + it)| > r_n - \varepsilon r_n = \frac{1 - \varepsilon}{2n^\sigma}.$$

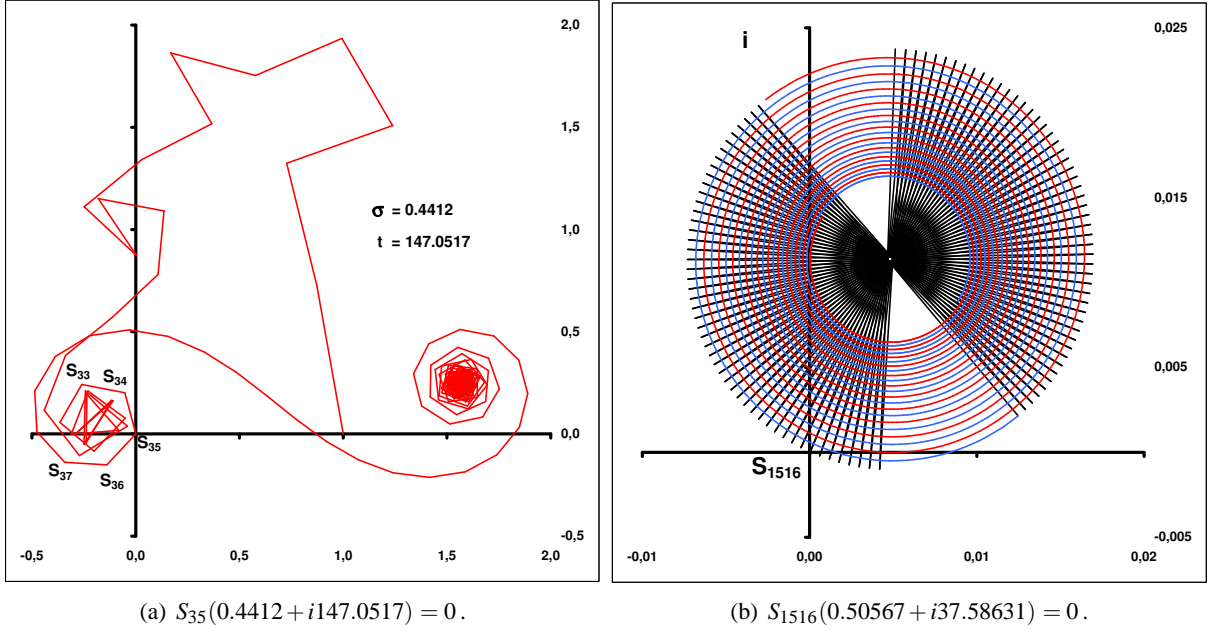
Choosing an index $m(s)$ such that $m > n_o(s)$ and $m > j(s)$, by combining (22) and (25) we finally have

$$\exists m = m(s) \in \mathbb{Z}^+ : \forall n > m \quad \frac{1 - \varepsilon}{2n^\sigma} < |R_n(\sigma + it)| < \frac{1}{n^\sigma}.$$

□

Definitions

Let us now introduce few definitions, later useful for writing in a simpler and more compact form the various statements.

Figure 4: $S_n(s) = 0$ examples.

a) As this work is concerned with the implications of the hypothetical existence of non-trivial zeros of $\zeta(s)$ located off the critical line, we will restrict our study to the open left half of the critical strip.

$$\text{Let } D \text{ be the domain } D = \left\{ s \in \mathbb{C} : 0 < \Re(s) < \frac{1}{2} \right\}.$$

Then remarking that the existence of zeros in D would naturally imply the existence of zeros also in the open right half critical strip (at locations symmetrical about the critical line).

b) The proof of Theorem 1 has shown that there exists an index $n_o(s)$ such that for all $n > n_o(s)$ the difference at the numerator of (18) is a strictly positive quantity. Such a condition corresponds to the disk built on *segment* $n+2$ being strictly contained inside the disk built on *segment* n .

Let $n_o(s)$ denote the index value such that $\forall n > n_o(s)$ the numerator of (18) is strictly positive .

c) For almost all s in the half plane $\Re(s) > 0$ there are no partial sums $S_n(s) = 0$. However, when there exist instances $S_n(s) = 0$, Corollary 1.2 will show that, for any given s , there could be at most one value $N(s) > n_o(s)$ corresponding to a vanishing partial sum.

When it exists, let $N(s)$ denote the only index value $N(s) > n_o(s)$ such that $S_N(s) = 0$.

d) We will also use the following definition for the limit of the sequence of functions $\{P_n(s)\}$.

For every $s \in D$ let $P_n(s) = S_n(1-s)/S_n(s)$. We define the limit $L(s)$, if it exists, as

$$L(s) = \lim_{N(s) < n \rightarrow \infty} P_n(s).$$

Corollary 1.1. *For any given $s \in D$, let us define $R_n(1-s)/R_n(s)$ as the ratio of the n^{th} residuals of the infinite series for $\eta(1-s)$ and $\eta(s)$. We have*

$$(26) \quad \lim_{n_o(s) < n \rightarrow \infty} \frac{R_n(1-s)}{R_n(s)} = 0 .$$

PROOF. The proof of **Theorem 1** shows that there exists an index $n_o(s)$ such that for all $n > n_o(s)$ a disk having *segment* $n+2$ as its diameter will be contained strictly inside a disk having *segment* n as its diameter, implying that as $n \rightarrow \infty$ the point of convergence, $\eta(s)$, is always contained strictly inside all of such nested disks. By observing that $R_n(s)$ corresponds, by definition, to one of the endpoints of *segment* n , it is clear that $R_n(s) \neq 0$ for all $n > n_o(s)$. Recalling (14), with $\alpha = \frac{1}{2} - \sigma$, we have

$$\lim_{n_o(s) < n \rightarrow \infty} \frac{R_n(1-s)}{R_n(s)} = \lim_{n_o(s) < n \rightarrow \infty} O(n^{-2\alpha}) = 0.$$

□

A further implication of **Theorem 1** is that for any given value of s , $\Re(s) > 0$, there can only be a finite number of partial sums such that $S_n(s) = 0$. In this respect, it shall be remarked that for almost all values of s none of the partial sums $S_n(s)$ will vanish. However, there certainly exist values of s corresponding to $S_n(s) = 0$, and Fig. 4 depicts two examples of just such cases. Each vertex of the depicted paths represents the value of a partial sum. Fig. 4a is an example whereby one of the partial sums (S_{35}) vanishes before the path has settled into its *star-shaped bound orbit*. While Fig. 4b is an example whereby one of the partial sums (S_{1516}) vanishes after the path has already settled into its *star-shaped bound orbit*. The two nested spiral patterns represent a different way to visualize the path followed by the partial sums: the red spiral is drawn by joining consecutive partial sums of even index (i.e.: the sums S_{2n}), while the blue spiral is drawn by joining consecutive partial sums of odd index (i.e.: the sums S_{2n+1}). For n ranging from 1501 to 1601 the path is drawn by joining consecutive values of the partial sums (the spiky black pattern). For better readability, starting at $n = 1601$, and up to $n = 10000$, said path is then split into a path composed of line segments with endpoints S_{2n} and S_{2n+2} , and a path composed of line segments with endpoints S_{2n+1} and S_{2n+3} . Thus resulting in the red and blue spirals.

Corollary 1.2. For any given $s \in \mathbb{C} : 0 < \Re(s)$, denoted by $S_n(s)$ the n^{th} partial sum of the series for $\eta(s)$, and by $\{k(s)\}$ the set of indexes for which $S_k(s) = 0$, we have that $\{k(s)\}$ can contain at most finitely many elements.

PROOF. Once the angle $\delta_n = t \ln \frac{n}{n-1}$ between two consecutive segments has become $< \frac{\pi}{2}$, the expression at the numerator of (18) can be used to compute the exact value of the index $n_o(s)$ such that for all $n > n_o(s)$ a disk having *segment* $n+2$ as its diameter will be contained strictly inside a disk having *segment* n as its diameter. Considering the possibility that some of the sums $S_n(s)$ might vanish for some index $k < n_o(s)$, it is trivial to observe that the number of such occurrences cannot certainly be more than n_o , and hence a finite value. But what about the possible number of such occurrences when $n > n_o$? Because, by definition, the end points of the line segments coincide with the sums $S_n(s)$, the fact that said disks are contained the second next one strictly inside the current one also implies that $S_{2n}(s) \neq S_{2m}(s)$ and $S_{2n+1}(s) \neq S_{2m+1}(s)$, whenever $n \neq m$, $2n, 2m > n_o$. Recalling that $S_{2n+1}(s) = S_{2n}(s) + 1/(2n+1)^s$, it must in addition be $S_{2n+1}(s) \neq S_{2n}(s)$. In other words, even-indexed sums eventually differ one from each other, odd-indexed sums also differ one from each other, and odd-indexed sums differ from even-indexed ones. Hence, we finally obtain

$$(27) \quad n, m > n_o(s), n \neq m \Rightarrow S_n(s) \neq S_m(s).$$

Therefore, if there exists an index $N(s) > n_o(s)$ such that $S_N(s) = 0$, then it must be the only one, as all other sums $S_n(s)$ will necessarily have different values. □

We are now armed with all the tools required to prove that the limit function $L(s)$ actually exists.

Corollary 1.3. The limit $L(s)$ exists on all D . Moreover

$$\text{if } \eta(s) = 0 \text{ then } L(s) = 0.$$

PROOF. On the domain D the sequences $S_n(s)$ and $S_n(1-s)$ are certainly convergent, to $\eta(s)$ and $\eta(1-s)$ respectively. **Corollary 1.2** proves that $S_n(s)$ is always $\neq 0$, but for a finite number of indexes n . Hence, if the limit $\lim_{n \rightarrow \infty} S_n(s)$ is also $\neq 0$ then $L(s)$ exists. But, what about the hypothetical case that $\lim_{n \rightarrow \infty} S_n(s) = 0$? In such a case, we already know that $\lim_{n \rightarrow \infty} S_n(1-s) = 0$ must also hold, suggesting that the limit of their ratio might possibly result in an undefined $\frac{0}{0}$ case. However, thanks to the peculiar

properties of convergence of the partial sums of the series for $\eta(s)$, this is not the case. Indeed, recalling that $\lim_{n \rightarrow \infty} S_n(s) = 0$ by definition implies $|S_n(s)| = |R_n(s)|$ (eqn. (12)), **Corollary 1.1** proves that $L(s)$, which can now be written as $L(s) = \lim_{n_o(s) < n \rightarrow \infty} R_n(1-s)/R_n(s) = 0$, would exist even in such case. \square

The result of **Corollary 1.2** applies point wise to any s in the half plane $0 < \Re(s)$, it is however possible to find related results applicable to compact subsets of said half plane.

Corollary 1.4. *In the half plane $0 < \Re(s)$, for every compact subset C that does not include zeros of $\eta(s)$ it is possible to find an index $N > 0$, independent from s , such that for all $s \in C$*

$$n > N \quad \Rightarrow \quad S_n(s) \neq 0 .$$

PROOF. Let $s = \sigma + it$ be a complex number in C . By choosing an index $n_o(s)$ such that the angle between *segment* $n_o(s)$ and *segment* $n_o(s)+1$ is $< \frac{\pi}{2}$, AND the expression at the numerator of (18) is > 0 , will guarantee that the path described by the sums $S_n(s)$ has already settled into a pattern characterized by the disk having *segment* $n+2$ as its diameter is contained strictly inside the disk having *segment* n as its diameter. Let us further choose an index $N(s) > |\eta(s)|^{-1/\sigma}$, and which shall also be $N(s) > n_o(s)$, so that it is certainly $|R_N(s)| < 1/N(s)^\sigma$. We finally have $|R_N(s)| < |\eta(s)|$, meaning that for $n > N(s)$ none of the $|S_n(s)| = |\eta(s) - R_n(s)|$ can vanish. For every $s \in C$ the corresponding $N(s)$ can only be a finite number, it is therefore sufficient to choose $N = \text{MAX}_C \{N(s)\}$. \square

The result of **Corollary 1.4** cannot be applied to compact subsets which contain zeros of $\eta(s)$. In such case, and once the path described by the sums $S_n(s)$ has already settled into a pattern characterized by the disk having *segment* $n+2$ as its diameter contained strictly inside the disk having *segment* n as its diameter, while s approaches a value corresponding to $\eta(s) = 0$ the value of the index n at which $S_n(s)$ could possibly vanish grows larger and larger as s gets closer and closer to said zero. This results from the fact that as $\eta(s)$ approaches zero the possibility of existence of a partial sum $S_n(s) = 0$ depends on whether $|R_n(s)| \approx |\eta(s)|$. Recalling that $|R_n(s)|$ is eventually $\Theta(\frac{1}{n^\sigma})$, and that in a small neighborhood of any point s by definition σ can only change by a correspondingly small amount, when $|R_n(s)|$ needs to be smaller and smaller the corresponding value of n needs to grow larger and larger. It can further be remarked that if the values n for which $|R_n(s)| \approx |\eta(s)|$ grow larger, then the spacing between consecutive vertexes (see for example those vertexes in Fig.4b) becomes smaller, thus increasing the chances for the actual existence of instances $S_n(s) = 0$. In other words: in D , zeros of $\eta(s)$ probably act as kind of "points of accumulation" for the zeros of the partial sums $S_n(s)$.

It is instead possible to prove the following result:

Corollary 1.5. *In the half plane $0 < \Re(s)$, for every compact subset C containing zeros of $\eta(s)$ it is possible to find an index $N_o > 0$, independent from s , such that for all $s \in C$ there can be at most one index $N(s) > N_o$ at which $S_N(s) = 0$. Moreover, for s such that $\eta(s) = 0$ it holds $S_n(s) \neq 0$ for all $n > n_o(s)$.*

PROOF. As in the proof of **Corollary 1.2**, once the angle $\delta_n = t \ln \frac{n}{n-1}$ between two consecutive segments has become $< \frac{\pi}{2}$, the expression at the numerator of (18) can be used to compute the exact value of the index $n_o(s)$. By choosing $N_o = \text{MAX}_C \{n_o(s)\}$, (27) proves that for any given $s \in C$ there can be at most only one index $N(s) > N_o$ such that $S_N(s) = 0$. When s is such that $\eta(s) = 0$, it follows $|S_n(s)| = |R_n(s)|$. The proof of **Corollary 1.1** then shows how $R_n(s) \neq 0$ for all $n > n_o(s)$. \square

Finally, a result holding on every compact subset regardless of whether or not it contains zeros:

Corollary 1.6. *In the half plane $0 < \Re(s)$, for every compact subset C it is possible to find an index $N_o > 0$, independent from s , such that for all $s \in C$*

$$n, m > N_o, n \neq m \quad \Rightarrow \quad S_n(s) \neq S_m(s) .$$

PROOF. The meaning of N_o is the same as introduced in the proof of **Corollary 1.5**. Recalling then (27), the above statement is immediately proved. \square

3. THE RIEMANN HYPOTHESIS

Theorem 2. *The statement that the limit function $L(s)$ is continuous on D is a necessary and sufficient condition for the following inequality to be satisfied in D*

$$(28) \quad \eta(s) \neq 0.$$

PROOF. **Corollary 1.3** proves that the limit function $L(s)$ exists on all D . Were the above inequality satisfied, it would hence follow that the equality

$$L(s) = \lim_{N(s) < n \rightarrow \infty} P_n(s) = \lim_{N(s) < n \rightarrow \infty} \frac{S_n(1-s)}{S_n(s)} = \frac{\lim_{N(s) < n \rightarrow \infty} S_n(1-s)}{\lim_{N(s) < n \rightarrow \infty} S_n(s)} = \frac{\eta(1-s)}{\eta(s)}$$

is certainly verified on all D . The functional equation further tells us that the right-hand side ratio of two functions, coinciding with the function $P(s)$ introduced at (10), is a continuous function. Hence, the limit function $L(s)$ would also be a continuous function.

It is now left to prove that were inequality (28) not true, then $L(s)$ would be discontinuous. To this end we first show how

$$P(s) = \frac{1-2^s}{1-2^{1-s}} 2(2\pi)^{-s} \cos\left(\frac{\pi}{2}s\right) \Gamma(s)$$

is a strictly positive function on D . Let us hence evaluate the zeros of the first factor

$$(29) \quad \frac{1-2^s}{1-2^{1-s}},$$

which is $= 0 \iff \Re(s) = \frac{1}{2}$ and $t = n \frac{2\pi}{\ln 2}$ ($n \in \mathbb{Z}$). For $s \in D$ it is therefore always $\neq 0$.

For the second factor we have

$$2(2\pi)^{-s} \neq 0$$

while for the third factor it is

$$\left| \cos\left(\frac{\pi}{2}(s)\right) \right| \geq \left| \sinh\left(\frac{\pi}{2}t\right) \right| > 0 \quad \text{when } t > 0$$

Because the Gamma function has no zeros [11], it is proved that $P(s)$ is a strictly non vanishing function on D . Recalling then **Corollary 1.3**, we finally have

$$\begin{aligned} \eta(s) \neq 0 &\Rightarrow L(s) = P(s) \\ \eta(s) = 0 &\Rightarrow L(s) = 0. \end{aligned}$$

It is therefore clear how the actual existence of any such hypothetical off-the-critical-line zeros would result in a discontinuity of the limit function $L(s)$. \square

By observing that said discontinuity can only be $L(s) = 0$, it is straightforward to derive the following Corollaries:

Corollary 2.1. *The Riemann Hypothesis is equivalent to the statement $L(s) \neq 0$ on D .*

The problem of proving that the properties of convergence of the partial sums $S_n(s)$ imply $\eta(s) \neq 0$ is therefore turned into the problem of proving that the "relative" properties of convergence of the $S_n(s)$'s "with respect to" the $S_n(1-s)$'s imply $L(s) \neq 0$.

Corollary 2.2. *The Riemann Hypothesis is equivalent to the statement $L(s) = P(s)$ on all D .*

Remarks.

As a useful exercise, the interested reader might further wish to verify that on the critical line it is $|P(\frac{1}{2} + it)| = 1$. To this end, note that the factor (29) turns into the ratio of a complex number with its conjugate, and so its modulus is $= 1$. Recalling a known relationship satisfied by the Gamma function,

$|\Gamma(\frac{1}{2} + it)| = \sqrt{\pi / \cosh(\pi t)}$ [12], and further observing that the complex cosine factor can be rewritten as

$\cos(\frac{\pi}{2}(\frac{1}{2} + it)) = \cos \frac{\pi}{4} \cosh(\frac{\pi}{2}t) + i \sin \frac{\pi}{4} \sinh(\frac{\pi}{2}t)$, (9) correctly simplifies to

$$1 \cdot \frac{2}{\sqrt{2\pi}} \cdot \frac{\sqrt{2}}{2} \sqrt{\cosh(\pi t)} \cdot \sqrt{\frac{\pi}{\cosh(\pi t)}} = 1$$

We can also remark how the result obtained by Saidak and Zvengrowski [10] proves that in D , and along directions parallel to the real axis, $|P(s)|$ is a monotonic function. In their Theorem 1 the two authors proved that the ratio of the modulus of Riemann Zeta Function values of critical line symmetrical arguments (named $\alpha(\Delta, t)$ in their article, but here renamed $a(\alpha, t)$ for consistency with symbols already used) is a strictly monotone increasing function of $\alpha = \frac{1}{2} - \Re(s)$, for $t \geq 2\pi + 1$ and $0 \leq \alpha \leq \frac{1}{2}$. It is easy to verify how the function plotted in Fig.2 relates to the ratio $a(\alpha, t)$ studied in [10]:

$$(30) \quad \left| \frac{\eta(\frac{1}{2} + \alpha + it)}{\eta(\frac{1}{2} - \alpha + it)} \right| = \left| \frac{1 - 2^{\frac{1}{2} - \alpha + it}}{1 - 2^{\frac{1}{2} + \alpha - it}} \right| \frac{1}{a(\alpha, t)}.$$

By means of simple algebra it can further be verified that:

$$(31) \quad \frac{\partial}{\partial \alpha} \left| \frac{1 - 2^{\frac{1}{2} - \alpha + it}}{1 - 2^{\frac{1}{2} + \alpha - it}} \right| \begin{cases} < 0 & \text{if } 0 \leq \alpha \leq \frac{1}{2} & t \neq n \frac{2\pi}{\ln 2} \\ = 0 & \text{if } \alpha = \frac{1}{2} & t = n \frac{2\pi}{\ln 2} \end{cases},$$

and so proving that, for $0 \leq \alpha \leq \frac{1}{2}$, $\left| \frac{1 - 2^{\frac{1}{2} - \alpha + it}}{1 - 2^{\frac{1}{2} + \alpha - it}} \right|$ is a monotone decreasing function of α . Because the product of two monotone decreasing functions, and both of which are positive, is also a monotone decreasing function, the result proved by Theorem 1 in [10] confirms that, for $t \geq 2\pi + 1$ and $0 \leq \alpha \leq \frac{1}{2}$, $|P(s)|$ is a strictly monotonically decreasing function of α . Furthermore, fixed a value $t \geq 2\pi + 1$, $|P(s)|$ has its maximum at $|P(\frac{1}{2} + it)| = 1$ and its minimum at $|P(it)| \geq 0$, whereby said minimum may vanish only when $t = n \frac{2\pi}{\ln 2}$.

4. CONCLUSIONS

An effective way to visualize in one's mind the result of **Theorem 2** is the following:

The limit function $L(s)$ exists regardless of whether or not the RH is true. If the RH is true, then $L(s)$ is a continuous function and its modulus is the function plotted in Fig. 2. If the RH is not true, then $L(s)$ still coincides with the function whose modulus is plotted in Fig. 2, excepts at the locations of the off-the-critical-line zeros, where it will feature discontinuities $L(s) = 0$.

The natural continuation of this work would then aim to verify whether said hypothesis of continuity could represent an easier challenge than the Riemann Hypothesis, or a more difficult one, or whether it would simply turn the RH into an equally difficult task. The author has set for himself the following plan for future research on this fascinating subject, while hoping that also other scholars might be interested in carrying this work further.

a) The last part of the Introduction has highlighted how the continuity of $L(s)$ would follow if it could be proved that the sequence of functions $\{P_n(s)\}$ is indeed *locally uniformly convergent*. So, besides trying tests for continuity, one might also try tests for uniform convergence. By observing that a hypothetical non-continuity of the limit function $L(s)$ would necessarily imply non-uniform convergence, one might try to verify in a more rigorous manner whether the pattern of convergence conjectured in Fig.9b is indeed representative of the most general *non-uniformly convergent* case.

b) The hypothetical *non-uniform* pattern of convergence depicted in Fig. 9b shows that the functions $|P_n(s) - P_m(s)|$, $|P_o(s) - P_n(s)|$ and $|P_o(s) - P_m(s)|$, all change sign at least twice. If it could then be demonstrated that there exists an index $N > 0$ such that for all $n, m > N$, $n \neq m$, the inequality $|P_n(s)| \neq |P_m(s)|$ is verified for all values of α but at most one (meaning: as α varies from 0 to $1/2$, while t is held fixed), then said *non-uniform* pattern of convergence would not be possible. Actually, the typical pattern of convergence depicted in Fig. 9a suggests that a weaker condition might suffice. As it can be observed, $|P_{1999}(s)| \geq |P(s)|$, whereas $|P_{2000}(s)| \leq |P(s)|$, with the equal sign holding at $s = \frac{1}{2} + it$, where,

by definition, $|P_n(\frac{1}{2} + it)| = 1$ for all n . Such a behavior, characterized by the ratios $|P_n(s)|$ "jumping" from one side of $|P(s)|$ to the other, as index n is incremented to $n + 1$, is very typical for almost all n . An intuitive explanation for this kind of behavior can be given by referring to Fig.4b, while choosing to define $0.50567 + i37.58631 = \frac{1}{2} + 0.00567 + i37.58631 = 1 - \bar{s}$, where $s = \frac{1}{2} - 0.00567 + i37.58631$. If we take for example $S_{1518}(1 - \bar{s})$ (i.e.: the next clockwise vertex from $S_{1516}(1 - \bar{s})$), we can see that $S_{1518}(1 - \bar{s}) \neq 0$, and that $S_{1518}(1 - \bar{s})$ is closer to 0 than $\eta(1 - \bar{s})$. The next partial sum, $S_{1519}(1 - \bar{s})$, is instead located much farther apart from 0 than $\eta(1 - \bar{s})$ (being located at a position almost diametrically opposed with respect to $\eta(1 - \bar{s})$). If we now imagine to represent in the same figure also $\eta(s)$, it is clear that $\eta(s)$ will be located farther apart from 0 than $\eta(1 - \bar{s})$ (because $|P(s)| < 1$). Considering then that the paths corresponding to $\eta(1 - \bar{s})$ and $\eta(s)$ are composed of parallel line segments (recall the example of Fig.1), and hence drawing very similar *star-shaped bound orbit*, it is not difficult to see how it may well happen that, for $0 < \sigma < \frac{1}{2}$, $|S_n(1 - \bar{s})|/|S_n(s)| < |\eta(s)|/|\eta(1 - \bar{s})|$, while $|S_{n+1}(1 - \bar{s})|/|S_{n+1}(s)| > |\eta(s)|/|\eta(1 - \bar{s})|$, or vice versa. Going back to Fig. 9a, let us choose to draw in red the ratios $|P_n(s)|$ of odd index, and in dark blue the ones of even index. By incrementing n we would observe the following pattern of convergence: for $n = 1999$ the red curve is above $|P(s)|$, while the blue one is below it; increasing n would bring the two curves close to each other, until, at $n = 2015$, both of them overlap the curve for $|P(s)|$ almost perfectly; further incrementing n would then result in said curves crossing over each other; at $n = 2029$ we would observe the red curve at its maximum deviation below $|P(s)|$, mirrored by a similar behavior of the blue curve from above $|P(s)|$; keeping incrementing n would then result in both curves drifting again towards $|P(s)|$; at $n = 2043$ they would cross again, with the red one drifting above $|P(s)|$, and the blue one drifting below it; and so on in apparently never ending cycles, with said maximum deviations from $|P(s)|$ getting smaller and smaller at each consecutive cycle. Denoted by C_t a subset of D defined by a fixed value of t , the just described asymptotic behavior suggests that there might exist infinitely many indexes $m > N_o$ (N_o with the same meaning as in **Corollary 1.5**), such that for every $s \in C_t$ it holds $|P_m(s)| < |P(s)|$. If we could then prove that chosen such an index $m > N_o$ the ratios $|P_n(s)|$, $n = m + j$, never cross $|P_m(s)|$, at least eventually as $j \rightarrow \infty$, then the hypotheticalal pattern of convergence depicted in Fig. 9b would not be possible, thus proving the Riemann Hypothesis.

It is further useful to remark that hypothetical locations at which the function $|P_n(s)| - |P_m(s)|$ might vanish (i.e.: the curve $|P_n(s)|$ crosses the curve $|P_m(s)|$) would be located at a distance greater than some value $\delta > 0$, no matter how small, from the location of a hypothetical zero, and hence in a region where the convergence of both the sums $S_n(s)$ AND the ratios $P_n(s)$ is locally uniform. The study of $|P_n(s)| \neq |P_m(s)|$ would be made simpler if it could be turned into the study of $P_n(s) \neq P_m(s)$. Although $|P_n(s)| \neq |P_m(s)|$ implies $P_n(s) \neq P_m(s)$, the converse is not true in general. However, given the pattern of convergence illustrated in Fig.4b, and which would be characteristic of both $S_n(s)$ and $S_n(1 - \bar{s})$ (their respective line segments being parallel to each other, as already explained for the example in Fig.1), the peculiar properties of convergence of the ratios $P_n(s)$ can probably allow to demonstrate that $|P_n(s)| \neq |P_m(s)| \Leftrightarrow P_n(s) \neq P_m(s)$, at least for almost all n . Proving that would in turn allow us to focus on the study of the inequality $S_n(1 - s) S_m(s) \neq S_n(s) S_m(1 - s)$, which simplifies to $(n = m + j)$:

$$S_m(s) \sum_{k=m+1}^{m+j} \frac{(-1)^{k-1}}{k^{1-s}} \neq S_m(1-s) \sum_{k=m+1}^{m+j} \frac{(-1)^{k-1}}{k^s} .$$

It is interesting to remark how, when $m > N_o$, $\Delta_{m+j}(s) = \left| \sum_{k=m+1}^{m+j} (-1)^{k-1} k^{-s} \right|$ represents the distance between two, vertex $S_m(s)$ and vertex $S_{m+j}(s)$, of the vertexes making up the *star-shaped bound orbit*. It is therefore likely that $\Delta_{m+j}(\sigma + it) = \Theta(m^{-\sigma})$. It can further be observed how $\Delta_{m+j}(s) \rightarrow |R_m(s)|$ as $j \rightarrow \infty$.

c) By looking at Fig.9, one might also wish to verify whether the properties of convergence of the sequence of functions $\{P_n(s)\}$ imply that there exists an index $N > 0$ such that

$$n > N \Rightarrow \frac{\partial}{\partial \alpha} P_n\left(\frac{1}{2} - \alpha + it\right) \neq 0 .$$

d) In Fig.9, while approaching the location $\alpha = 0.15$ of the hypothetical zeros, the $\frac{\partial}{\partial \alpha} |P_n(\frac{1}{2} - \alpha + it)|$ grows larger and larger, as $n \rightarrow \infty$, before sharply decreasing again to vanish at $\alpha = 0.15$. This observation suggests that one might also try to verify whether it exists an upper bound $M > 0$ no matter how large, and an index $N \in \mathbb{Z}+$ such that

$$n > N \Rightarrow \frac{\partial}{\partial \alpha} \left| P_n\left(\frac{1}{2} - \alpha + it\right) \right| < M .$$

e) One might wish to try all of the above also for cross-sections along t , while α is held fixed (as for example in Fig. 5a and 5b). Of course, more caution will be needed, as now the corresponding $|P_n(\frac{1}{2} - \alpha + it)|$, would feature minima and maxima even for the case of uniform convergence, although probably of a type clearly discernible from the one expected for a non-uniform convergence behavior of the type exemplified in Fig.9. The discussion following **Conjecture 1** shows that such inherent minima and maxima would be countable, occurring at integer multiples of $t = \pi/\ln 2$ or very close to it, and in any case at the rate of one maximum and one minimum every $t = 2n\pi/\ln 2$, however their actual spacing inside such $\Delta t = 2\pi/\ln 2$ intervals may be. In such case, if it could in addition be demonstrated that the number of instances $\frac{\partial}{\partial t} |P_n(\frac{1}{2} - \alpha + it)| = 0$ cannot be larger than said countable infinity (for example by proving that there could only be one maxima and one minima in each of the consecutive intervals of width $\Delta t = 2\pi/\ln 2$), that would suffice to exclude non-uniform convergence.

Whether we are studying the behavior along the α or the t direction, any hypothetical "signature" of non-uniform convergence would need to occur at the same pair of α, t values.

5. APPENDIX

The 2D plots of Fig. 5 depict some relevant sections of the 3D plot of Fig.2. Concerning the "wavy" pattern visible in Fig. 5a and 5b, the "deeps" correspond to even multiples of $t = \pi/\ln 2$, while the points of contact with the upper bound curve appear to take place at odd multiples of $t = \pi/\ln 2$. In Fig. 5c and 5d the small red dots (visible in the electronic version of this article, by zooming in as necessary) represent values of $|\eta(\frac{1}{2} + \alpha + it)/\eta(\frac{1}{2} - \alpha + it)|$.

Within the available resources, the author has not yet been able to verify in a more analytical way the results summarized in the plots of Fig. 2 and 5. Therefore, at the time of writing (7) cannot be considered more than just a conjecture, perhaps useful for inspiring some future work on the subject.

REFERENCES

- [1] Riemann, Bernhard. Über die Anzahl der Primzahlen unter einer gegebenen Grösse. The Clay Mathematical Institute (2000). PDF copy of the original
- [2] Derbyshire, John. Prime Obsession: Bernhard Riemann and the Greatest Unsolved Problem in Mathematics, page 191. Penguin Group, New York (2004)
- [3] Weisstein, Eric W. "Riemann Hypothesis." From MathWorld—A Wolfram Web Resource. mathworld.wolfram.com/RiemannHypothesis.html
- [4] Bombieri, Enrico. The Riemann Hypothesis—official problem description. The Clay Mathematical Institute (2000). The Official Problem Description
- [5] Sarnak, Peter. Problems of the Millennium: The Riemann Hypothesis. The Clay Mathematical Institute (2004). The Riemann Hypothesis
- [6] Sondow, Jonathan and Weisstein, Eric W. "Riemann Zeta Function." From MathWorld—A Wolfram Web Resource. mathworld.wolfram.com/RiemannZetaFunction.html
- [7] Weisstein, Eric W. "Riemann Zeta Function Zeros." From MathWorld—A Wolfram Web Resource. mathworld.wolfram.com/RiemannZetaFunctionZeros.html
- [8] Weisstein, Eric W. "Dirichlet Eta Function." From MathWorld—A Wolfram Web Resource. mathworld.wolfram.com/DirichletEtaFunction.html
- [9] Derbyshire, John. Prime Obsession: Bernhard Riemann and the Greatest Unsolved Problem in Mathematics, page 147. Penguin Group, New York (2004)
- [10] Saidak, Filip and Zvengrowski, Peter. On the Modulus of the Riemann Zeta Function in the Critical Strip, Mathematica Slovaca, **53** No.2, 145-172 (2003)
- [11] Morse, Philip M. and Feshbach, Herman. Methods of Theoretical Physics, page 420. McGraw-Hill Publishing Company, New York (1953)

- [12] Weisstein, Eric W. "Gamma Function." From MathWorld—A Wolfram Web Resource. mathworld.wolfram.com/GammaFunction.html
- [13] Abramovitz and Stegun. "Handbook of Mathematical Functions", par. 6.1.45 at pg. 257. Available online at UCLA.
- [14] Apostol Tom. Introduction to Analytic Number Theory, Theorem 11.11 at page 235. Springer, ISBN 0-387-90163-9

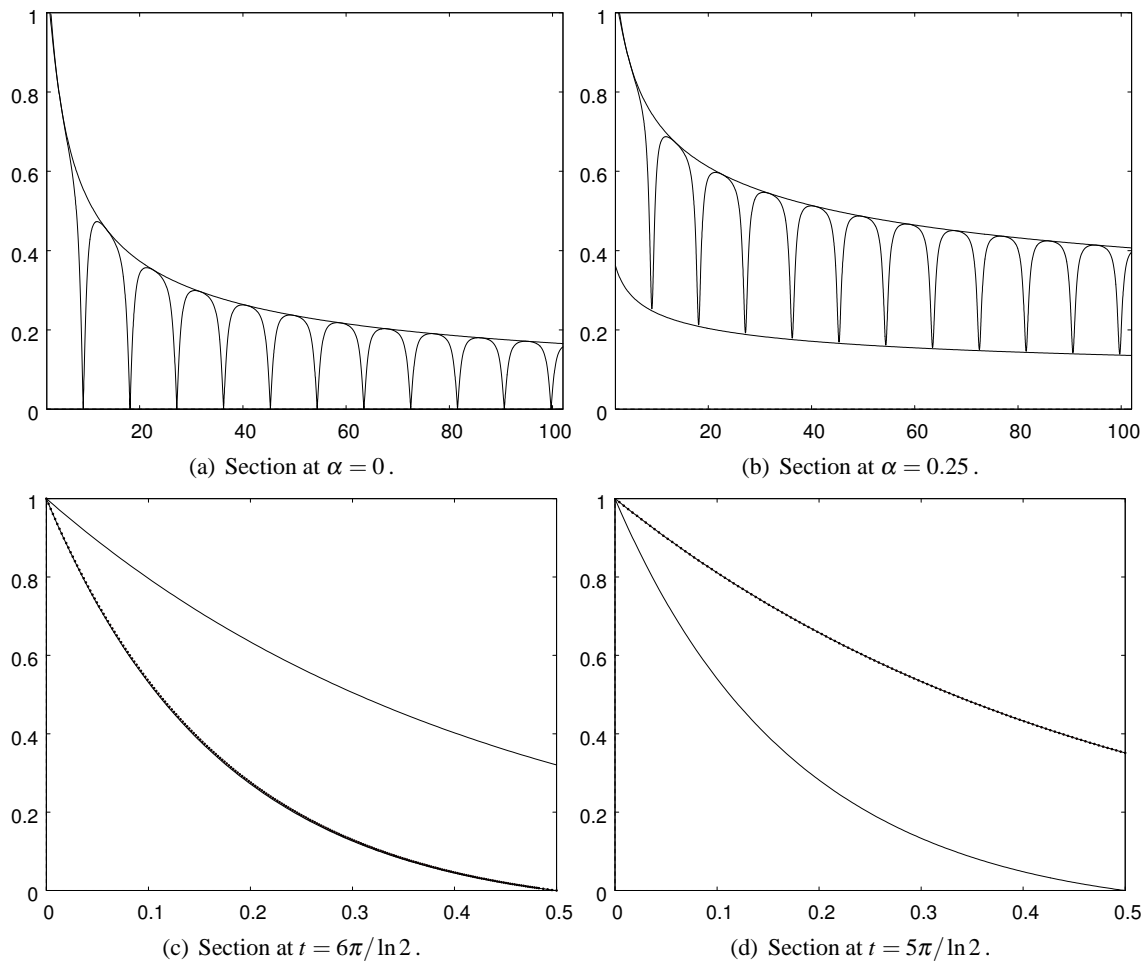
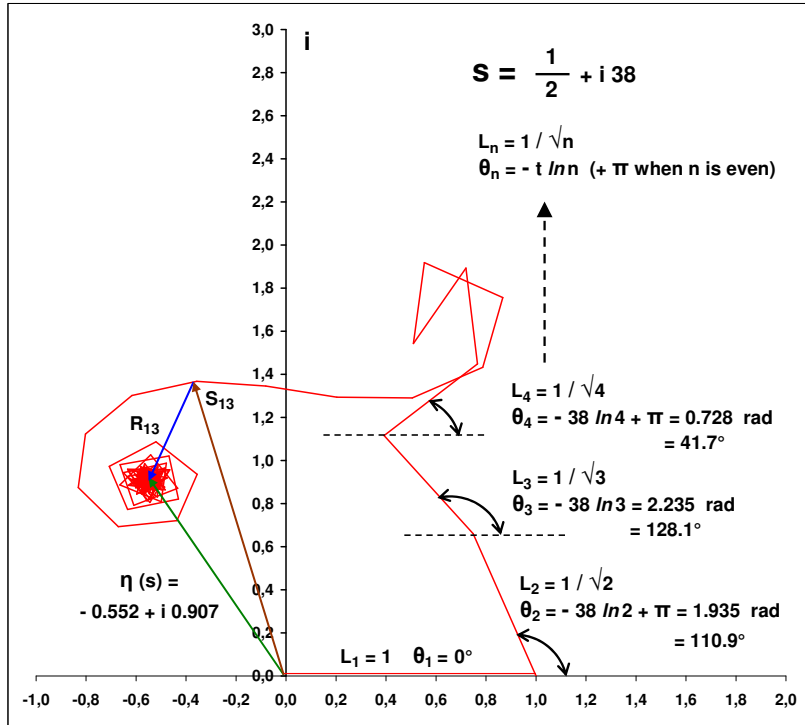
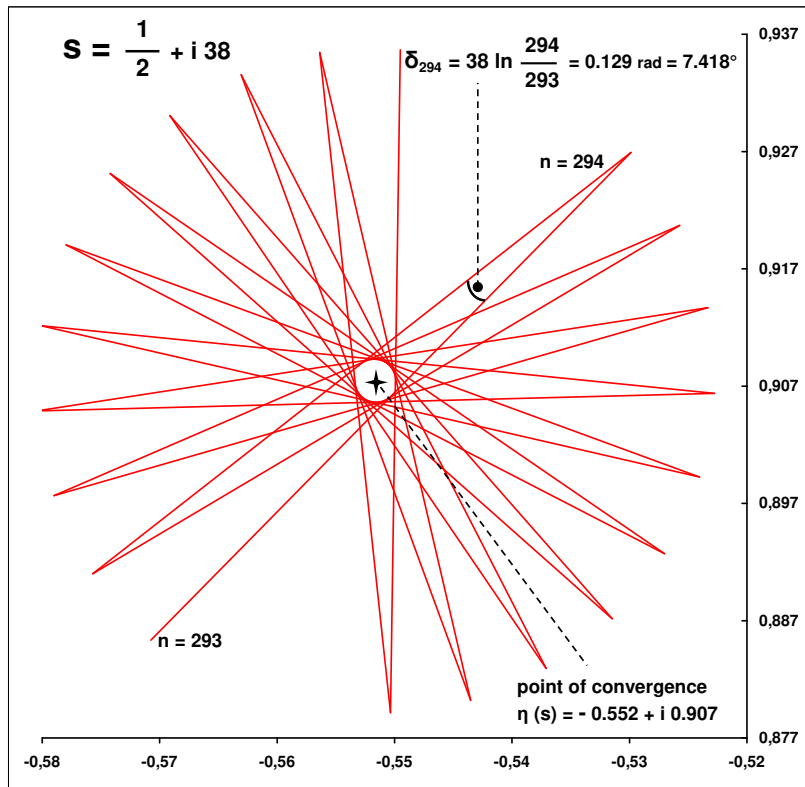


Figure 5: relevant 2D sections of the 3D plot of Figure 2.

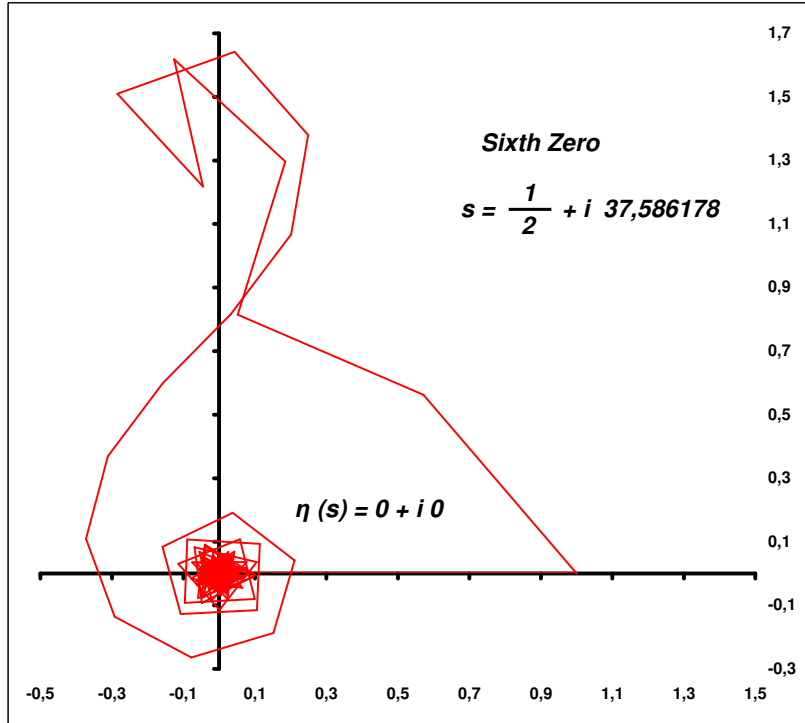


(a) Example corresponding to $\eta(1/2 + i38)$.

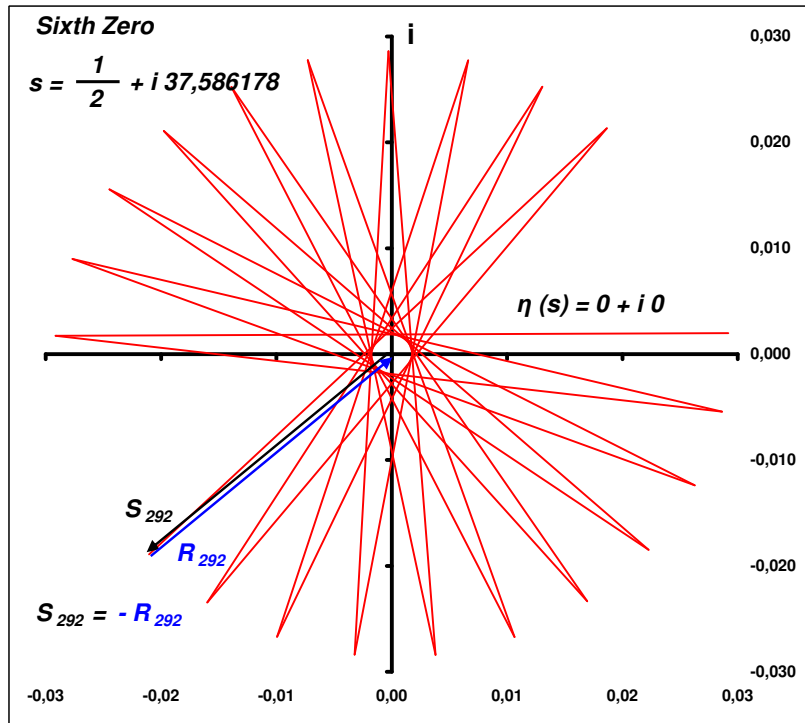


(b) Zooming on the segments from $n=293$ to $n=313$.

Figure 6: The path described by the partial sums of the series for $\eta(s)$.



(a) $\eta(1/2 + i37,586178)$.



(b) Zooming on the segments from $n=293$ to $n=313$.

Figure 7: The path corresponding to the sixth known zero.

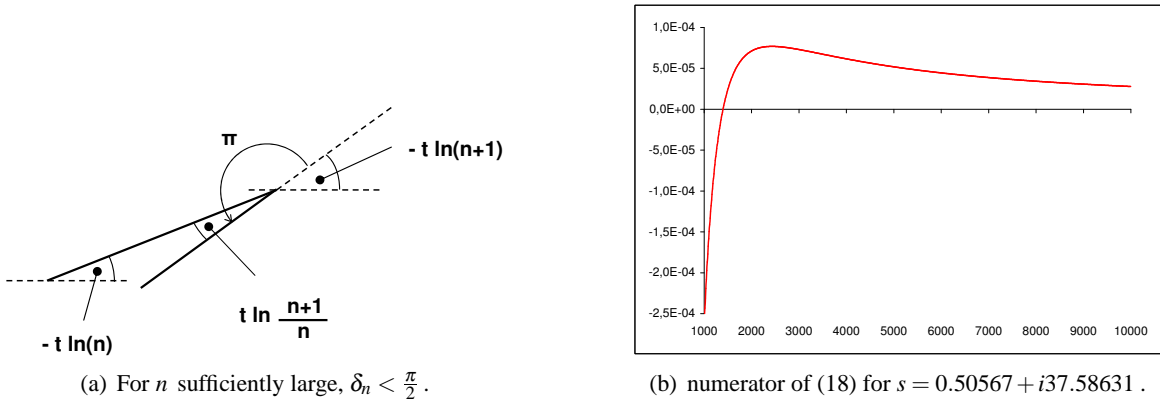
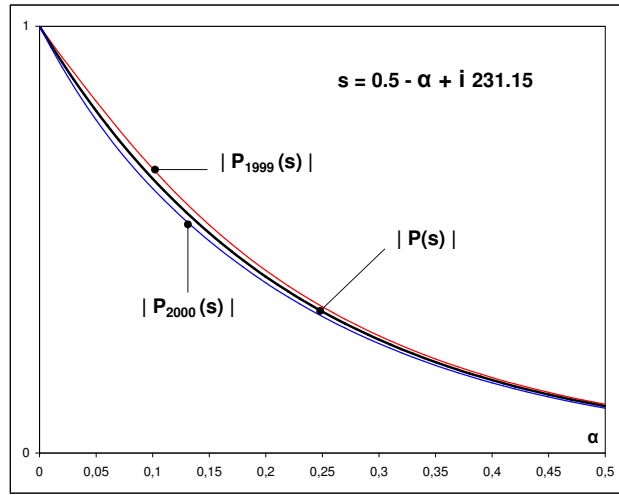
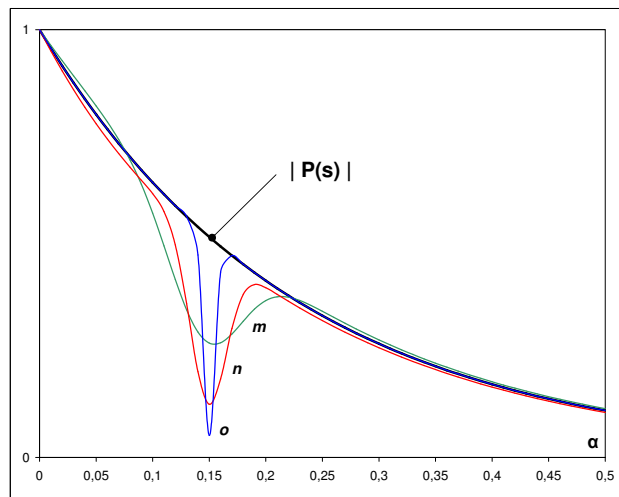


Figure 8:



(a) Typical.



(b) Expected in case of zeros at $\alpha = 0.15$.

Figure 9: Patterns of convergence of the ratios $|P_n(s)|$.